Integrated Transcriptomic and Metabolomic Analyses of the Molecular Mechanisms of Two Highland Barley Genotypes with Differential Pyroxsulam Responses

Hua Weng
Qinghai Academy of Agriculture and Forestry Sciences
Jiahui Yan (15209787170@163.com)
Qinghai Academy of Agriculture and Forestry Sciences
Liangzhi Guo
Qinghai Academy of Agriculture and Forestry Sciences
Hongyu Chen
Qinghai Academy of Agriculture and Forestry Sciences

Research Article

Keywords: flavonoids, antioxidants, transcriptome, metabolome, highland barley, pyroxsulam

Posted Date: September 20th, 2021

DOI: https://doi.org/10.21203/rs.3.rs-798616/v1

Abstract

Background: Highland barley is one of the few crops that can be grown at high elevations, making it a key resource within the Tibet Plateau. Weeds are a significant threat to highland barley production and new herbicides and tolerant barley varieties are needed to control this ever-growing problem.

Results: A better understanding of existing herbicide resistance mechanisms is therefore needed. In this study, transcriptomic and metabolomic analyses were used to identify molecular and physiological changes in two highland barley genotypes with differing sensitivities to pyroxsulam. We identified several stress-responsive metabolites, including flavonoids and antioxidants, which accumulated to significantly higher levels in the pyroxsulam-resistant genotype. Additionally, we found key genes in both the flavonoid biosynthesis pathway and the antioxidant system were up-regulated in pyroxsulam-resistant barley.

Conclusions: This work significantly expands on the current understanding of the molecular mechanisms underlying differing pyroxsulam tolerance among barley genotypes and provides several new avenues to explore for breeding or engineering tolerant barley.

1. Introduction

Highland barley (*Hordeum vulgare* L.) is an economically important crop and is the only cereal that can mature normally in the short growing seasons often found at high altitudes [1]. It is the fourth most important cereal crop worldwide and is primarily utilized for animal feed, brewing, distilling and malting [2]. However, highland barley remains a major food source in some areas, such as West Asia and North Africa [3]. Although it is grown throughout the world, the majority of its cultivation lies in East Asian countries, such as China, which produces 77% of the total highland barley grown worldwide [4]. Highland barley is also consumed as a staple crop in regions of the Qinghai-Tibet Plateau, including Sichuan, Gansu, Qinghai and Tibet. Highland barley is consumed in this region due to its health benefits, which stem from its metabolites, bioactive carbohydrates, polyphenols, vitamins, phenolic, flavonoids and β-glucans [5]. Additionally, research has indicated that highland barley may possess antihyperglycemic, antihyperlipidemic and anticancer activities [6]. Despite these benefits, there are several challenges in growing barley in the Tibet Plateau, including a high amount of invasive weeds. However, the highland barley is grown in the harsh environment of the Tibet Plateau, the yield and productivity are significantly impaired by troublesome weeds. There are many weeds and single herbicides in highland barley field, which is the main factor restricting the development of barley industry. The development of herbicide-resistant barley varieties is critical to increasing the production efficiency of this crop system by enabling the use of more efficient weed control systems.

Pyroxsulam is a new triazolopyrimidine sulfonamide acetolactate synthase (ALS)-inhibiting herbicide developed by Dow AgroSciences (Indianapolis, IN), which provides broad-spectrum control of many annual, biannual and perennial weeds. It has the advantage of high efficacy with low doses and a favorable environmental profile [7]. Pyroxsulam acts by inhibiting ALS, an important target for herbicides,

which is an essential enzyme that catalyzes the first step in the synthesis of the branched-chain amino acids valine, leucine and isoleucine [8]. The resulting lack of amino acids in the plant inhibits DNA synthesis, subsequently stopping cell division and causing death in susceptible plants [9]. Commercial formulations of pyroxsulam with the herbicide safener cloquintocet allow for selective weed control in cereal crops. Pyroxsulam is currently one of the most widely used herbicides in the world, but little is known about its effects on highland barley. A better understanding of the mechanisms underlying variable pyroxsulam tolerance among highland barley genotypes is critical to efficiently utilizing this herbicide in its production.

The success of breeding herbicide-tolerant varieties relies on the availability of tolerant locally adapted germplasm. Recently, the integration of various omics technologies has proven to be indispensable for determining potential tolerance mechanisms. We performed a comparative analysis of two highland barleys with differing tolerance to pyroxsulam and identified substantial differences in their metabolomes and transcriptomes. These differences included key genes in pathways associated with amino acid biosynthesis, reactive oxygen tolerance and flavonoids. These results showed that the profiled metabolic alterations in highland barley of a pyroxsulam- resistive and a pyroxsulam-sensitive, and have a reprogramming of the amino acids biosynthesis pathway toward the flavonoid pathway after treatment with herbicide pyroxsulam. Our results imply that pyroxsulam-tolerant highland barley varieties induce the expression of flavonoids and reactive oxygen species (ROS) scavengers enzymes in order to resist pyroxsulam toxicity. These results provide a good starting point for understanding highland barley pyroxsulam tolerance, although the underlying mechanisms behind these different responses are complex and require additional research. Our results provided deeper insights into the molecular mechanisms and candidate genes for further study and breeding the resistance against herbicide pyroxsulam in highland barley.

2. Materials And Methods

2.1 Plant material

Qing 0160 and Qing 0305 were collected from Xining City, Qinghai Province, China(N.36.434419,E.101.450759).The samples were identified by Liling Jiang and deposited at the National duplicate Genbank for crops, Xining, Qinghai province, China. The specimen accession number were ZDM1651 and ZDM 8091.

2.2 Sample preparation and RNA isolation

Two highland barley genotypes were used for this study, including one pyroxsulam-sensitive genotype and one insensitive genotype. All highland barley seedlings were grown in a potting medium under a 11 h light (25°C)/13 h dark (20°C) day/night cycle with 75% humidity. The pyroxsulam herbicide was applied during the two-leaf stage, with the typical field application concentration of 12.5 g/666.7 m^2. Leaf samples were harvested at 0, 1 and 6 days after treatment with pyroxsulam, then stored at − 80°C for

metabolite profiling and RNA-sequencing. Total RNA was isolated using an RNA extraction kit from (Sangon, Shanghai, China).

2.3 Library preparation for transcriptome sequencing

Total RNA was used as input material for the RNA sample preparations. Briefly, mRNA was purified from total RNA using poly-T oligo-attached magnetic beads. Fragmentation was carried out using divalent cations under elevated temperature in First Strand Synthesis Reaction Buffer (5X). First-strand cDNA was synthesized using a random hexamer primer and M-MuLV Reverse Transcriptase, followed by RNaseH RNA digestion. Second-strand cDNA synthesis was subsequently performed using DNA Polymerase I and dNTPs. The remaining overhangs were converted into blunt ends via exonuclease/polymerase activities. After adenylation of the 3’ ends of the DNA fragments, adaptors with hairpin loop structures were ligated to prepare for hybridization. In order to select cDNA fragments that were 370–420 bp in length, the library fragments were purified with the AMPure XP system (Beckman Coulter, Beverly, USA). Then, PCR was performed with Phusion High-Fidelity DNA polymerase, Universal PCR primers and an index (X) Primer. Finally, PCR products were purified using the AMPure XP system and library quality was assessed on the Agilent Bioanalyzer 2100 system.

2.4 Sequence data mapping and transcriptome analysis

Raw FASTQ formatted reads were first processed through in-house Perl scripts to generate clean reads, with adaptor sequences trimmed and reads containing Ns or low-quality bases removed. Scripts were then used to calculate Q20, Q30 and GC content. All the downstream analyses were based on clean data with only high-quality reads retained.

Reference genome and gene model annotation files were downloaded from a public database. The reference genome index was built using Hisat2 v2.0.5 and paired-end clean reads were aligned to the reference genome using Hisat2 v2.0.5.

2.5 Differential expression analysis

Differential expression analysis of the two conditions (three biological replicates per condition) was performed using the DESeq2 R package (1.20.0). The resulting *P*-values were adjusted using the Benjamini and Hochberg’s approach for controlling the false discovery rate. Genes with an adjusted *P*-value < 0.05 found by DESeq2 were considered differentially expressed.

2.6 GO and KEGG enrichment analysis of differentially expressed genes

Gene Ontology (GO) enrichment analysis of differentially expressed genes (DEGs) was implemented via the clusterProfiler R package. GO terms with corrected *P*-values less than 0.05 were considered significantly enriched. KEGG was employed to determine high-level function of DEGs (http://www.genome.jp/kegg/). We used the clusterProfiler R package to test the statistical enrichment of DEGs in KEGG pathways.

2.7 Metabolite extraction

Each sample consisted of 100 mg of tissue, which was ground with liquid nitrogen, followed by resuspension in prechilled 80% methanol and 0.1% formic acid by vortexing. The samples were incubated on ice for 5 min and then centrifuged at 15,000 rpm and 4°C for 5 min. Some of the supernatant was diluted to a final concentration containing 53% methanol with LC-MS grade water. The samples were subsequently transferred to a fresh Eppendorf tube and were then centrifuged at 15,000 g and 4°C for 10 min. Finally, the supernatant was injected into an LC-MS/MS system for analysis [1]. Liquid sample (100 μL) and prechilled methanol (400 μL) were mixed by vortexing [2–3]. Samples and prechilled 80% methanol were mixed by vortexing, and then sonicated for 6 min [4–5].

2.8 UHPLC-MS/MS analysis

UHPLC-MS/MS analyses were performed using a Vanquish UHPLC system (Thermo Fisher, Germany) coupled with an Orbitrap Q ExactiveTM HF mass spectrometer (Thermo Fisher, Germany) at the Novogene Co., Ltd. (Beijing, China). Samples were injected onto a Hypersil Gold column (100×2.1 mm, 1.9 μm) using a 17 min linear gradient at a flow rate of 0.2 mL/min. The eluents for the positive polarity mode were eluent A (0.1% FA in water) and eluent B (methanol). The eluents for the negative polarity mode were eluent A (5 mM ammonium acetate, pH 9.0) and eluent B (methanol). The solvent gradient was set as follows: 2% B, 1.5 min; 2-100% B, 12.0 min; 100% B, 14.0 min; 100-2% B, 14.1 min; and 2% B, 17 min. Q ExactiveTM HF mass spectrometer was operated in positive/negative polarity mode with spray voltage of 3.2 kV, capillary temperature of 320°C, sheath gas flow rate of 40 arb and aux gas flow rate of 10 arb.

2.9 Data processing and metabolite identification

The raw data files generated by UHPLC-MS/MS were processed using Compound Discoverer 3.1 software (CD3.1, Thermo Fisher) to perform peak alignment, peak picking and quantitation for each metabolite. The main parameters were set as follows: retention time tolerance, 0.2 minutes; actual mass tolerance, 5 ppm; signal intensity tolerance, 30%; signal/noise ratio, 3; and minimum intensity, 100,000. Next, peak intensities were normalized to the total spectral intensity. The normalized data were used to predict the molecular formula based on additive ions, molecular ion peaks and fragment ions. Peaks were then matched with the mzCloud (https://www.mzcloud.org/), mzVault and MassList databases to obtain accurate qualitative and relative quantitative results. Statistical analyses were performed using the statistical software R (R version R-3.4.3), Python (Python 2.7.6 version) and CentOS (CentOS release 6.6). When data were not normally distributed, normal transformations were attempted using the area normalization method.

3.0 Data analysis

Metabolites were annotated using the KEGG database (https://www.genome.jp/kegg/pathway.html), the human metabolome database (HMDB, https://hmdb.ca/metabolites) and LIPID Maps database (http://www.lipidmaps.org/). Principal component analysis (PCA) and partial least squares discriminant analysis (PLS-DA) were performed with MetaX. We applied univariate analysis (*t*-test) to calculate the statistical significance (*P*-value).

3. Results

3.1. Global transcriptomic difference in highland barley

In order to determine the different molecular mechanisms of two highland barley genotypes in response to pyroxsulam, we compared transcriptomic data at 0, 1 and 6 days after pyroxsulam treatment. Raw and clean reads were obtained from 18 samples using the Illumina sequencing platform (Table S1). We applied fragments per kilobase of transcript per million mapped reads (FPKM) to normalize the expression levels of the genes. The numbers of DEGs in highland barley with more than a 2-fold change in expression ($P < 0.05$) are shown in Table S2. The numbers of DEGs varied between treatment-by-time (Fig. 1A) and the volcano maps for all DEGs are shown in Fig. 1B-1D. Among the DEGs, the pyroxsulam without treatment resulted in the largest number of DEGs (6432 up-regulated and 6143 down-regulated genes in R0 vs S0) (Fig. 1B). One day after pyroxsulam treatment resulted in the smallest number of DEGs (2013 up-regulated and 2191 down-regulated genes in R1 vs S1) (Fig. 1C). The number of DEGs after 6 days of pyroxsulam exposure was slightly higher than 0 days after treatment (3967 up-regulated and 3869 down-regulated genes in R6 vs S6) (Fig. 1D). These results suggestion that pyroxsulam different treatment time showed different gene expression profiles.

3.2 Gene ontology (GO) enrichment analysis of DEGs

DEGs were subjected to GO enrichment analysis to identify enriched biological functions. Genes associated with small molecule metabolic process, carbohydrate metabolic process and organic acid metabolic process showed the greatest differential expression in the R0vsS0 group in the biological process (BP) category, while genes associated with NAD binding and oxidoreductase activity, acting on the aldehyde or oxo group of donors showed the greatest differential expression in the R0vsS0 group in the molecular function (MF) category. Genes associated with transferase activity, transferring glycosyl groups, transmembrane transporter activity and transferase activity, and transferring hexosyl groups showed the greatest differential expression in the R1vsS1 group in the MF category. Genes associated with small molecule metabolic process, cellular amide metabolic process and peptide metabolic process showed the greatest differential expression in the R6vsS6 group in the BP category. Genes associated with non-membrane-bounded organelle, intracellular non-membrane-bounded organelle and ribonucleoprotein complex showed the greatest differential expression in the R6vsS6 group in the cellular component (CC) category. Finally, genes associated with structural molecule activity, coenzyme binding and structural constituent of ribosome showed the greatest differential expression in the R6vsS6 group in the MF category (Fig. 2). These data indicate that there are significant differences in highland barley

resistant and sensitive varieties in a variety of biological processes, molecular functions and cellular components in response to pyroxsulam, which likely drive their different tolerances to this herbicide.

3.3 KEGG Pathway classification of DEGs.

To identify biological pathways related to DEGs, KEGG pathway analysis was performed. We found that the DEGs were associated with several enriched signaling pathways, including “Carbon metabolism”, “Biosynthesis of amino acids” and “Oxidative phosphorylation”, when comparing R0 to S0 (Fig. 3A). In the R1vsS1 group, the DEGs were associated with “Ribosome” and “Photosynthesis - antenna proteins” (Fig. 3B). In the R6vsS6 group, “Ribosome”, “Biosynthesis of amino acids” and “Carbon metabolism” were significantly enriched (Fig. 3C). These results indicated that metabolism, biosynthesis, modification and other pathways may be involved in these two genotypes’ differing tolerance to pyroxsulam. These gene expression differences highlight common responses to the pyroxsulam condition but also show that these genotypes differ substantially from each other.

3.4 Screening of Differential Metabolites of Highland Barley

Screening of differential metabolites of highland barley

Metabolomics is closer to phenotypic omics, and can be viewed as an extension of transcriptomics and proteomics that reflects the current physiological state of an organism. To compare the metabolic changes that took place after pyroxsulam treatment in tolerant and susceptible genotypes, we employed metabolomics. In total, 837 and 386 metabolites in the positive and negative ionization modes were detected and identified in all samples (Table S1 and S2). Volcano plots can be used to display the overall distribution of different metabolites, with the abscissa representing the differences in the changes of metabolites in different groups ($\log_2$FoldChange), and the ordinate representing the significance level of differences (-$\log_{10}$p-value). Each point in the volcano chart represents a different metabolite. The significantly up-regulated metabolites are represented by red dots, while the significantly down-regulated metabolites are represented by green dots, and the size of the dot represents the VIP value. After constructing a volcano plot, it could be seen that significantly more stress-responsive metabolites, including flavonoids and antioxidants, were identified in the pyroxsulam-resistant genotype compared to the pyroxsulam-sensitive genotype (Fig. 4).

3.5 Differential metabolite KEGG enrichment

To understand the metabolic activities of the two highland barleys after pyroxsulam treatment, we mapped the annotated metabolites to KEGG pathways. Enrichment analysis of the KEGG pathways can determine the main biological functions performed by the differential metabolites. According to the above enrichment results, a bubble chart of the top 20 enriched KEGG pathways was constructed (Fig. 5). A number of pathways were found to be differentially expressed, including “carbon metabolism”, “Phenylalanine metabolism”, “ABC transporters” and “Biosynthesis of amino acids” in the R0vsS0

comparison group (Figs. 5A and B). “Metabolic pathways”, “Tryptophan metabolism” and “Flavonoid biosynthesis” were found to have the greatest enrichment in the R1vsS1 group (Figs. 5C and D). Finally, “Biosynthesis of secondary metabolites” and “Flavonoid biosynthesis” were most significantly enriched in the R6vsS6 group (Figs. 5E and 5F). These metabolites cover most of central metabolism and reflect the physiological state. Taken together, these results show that flavonoid biosynthesis was consistently different in tolerant versus susceptible highland barley genotypes, indicating that it likely plays a central role in the differing tolerances of the two highland barley varieties.

3.6 Correlation between differential gene and differential metabolite expression

To understand the regulatory networks of the two highland barley genotypes’ responses to pyroxsulam, a correlation analysis was carried out with DEGs obtained by transcriptome analysis and the significantly different metabolites obtained by metabolomics analysis to construct an integrated metabolic map (Fig. 6). The map showed that the pathways involved in amino acid metabolism were enriched significantly without pyroxsulam treatment (R0 vs. S0) (Fig. 6A). The gene expression and metabolic flux shifted from amino acid metabolism to pyruvate metabolism and tropane, piperidine and pyridine alkaloid biosynthesis soon after pyroxsulam treatment (R1 vs. S1) (Fig. 6B). The genes involved in the phenylpropanoid and glutathione metabolic pathways were up-regulated, leading to the high accumulation of flavonoid and antioxidants after 6 days of pyroxsulam treatment (R6 vs. S6) (Fig. 6C). Overall, these results suggest that several genes encoding key enzymes involved in the biosynthesis process of flavonoids and other crucial metabolites were differentially expressed, suggesting that these genes could be valuable targets for improved pyroxsulam tolerance in highland barley.

Discussion

Weeds pose a significant threat to the production of highland barley, and new herbicides are required to deal with this ever-evolving problem [10]. Advances in biotechnology have led to the discovery of several herbicides that belong to different chemical classes and possess diverse modes of action. These newer herbicides represent the most cost-effective and environmentally sustainable way to control weeds and increase worldwide food production [11]. Previously, herbicides could only be applied to a limited number of crops but the development of herbicide-resistant varieties has greatly expanded their spectrum of use [12, 13]. Highland barley has not been extensively investigated for herbicide tolerance, which limits the herbicides that can be used to control weeds, thus limiting barley productivity. In this study, we utilized time-course metabolic profiling and transcriptional profiling of tolerant and sensitive highland barley accessions to better understand the mechanisms underlying their tolerance differences. An integrated analysis of the transcriptome and metabolome revealed significantly more stress-responsive metabolites in the pyroxsulam-resistant highland barley compared to pyroxsulam-susceptible. The up-regulation of key genes in the phenylpropanoid pathway led to flavonoid accumulation, which may represent a mechanism responsible for their differing tolerances. In addition, several unique metabolites and

unidentified compounds, such as glutathione, oxyresveratrol, artemtherin and others, could play a protective role during responses to pyroxsulam.

Metabolic reprogramming of the phenylpropanoid pathway has been reported to play a key role in response to biotic and abiotic stresses in rice, maize and soybean [14–16]. Metabolic profiling during fungal infection has shown a mobilization of carbohydrates, changes in amino acid pools, and the activation of flavonoid biosynthetic pathways in soybean [17]. Additionally, drought-stressed Arabidopsis has been reported to possess significantly different metabolite profiles, including large changes in flavonoids [18].

It has previously been reported that flavonoids play a major role in protection against stresses in plants. For example, flavonoids accumulate in maize plants growing at high altitudes to prevent damage caused by high UV-B exposure [19]. An increase in flavonoid secondary metabolites has also been shown to provide protection during pathogen infection [20]. Researchers have also reported that flavonoids are involved in the resistance to aluminum toxicity in maize [21]. Flavonoids have been shown to possess antimicrobial activity in plants, and have potent antifungal activity against several major plant fungal pathogens, including *Fusarium oxysporum* [22]. In the current study, we found that the biosynthesis of flavonoids significantly increased during pyroxsulam treatment, with pyroxsulam-tolerant barley showing a stronger induction. These results provide a starting point for using metabolomics to assist in the breeding of pyroxsulam-tolerant highland barley varieties.

Herbicides have been demonstrated to result in the generation of ROS in plants, with antioxidant systems often being responsible for the tolerance level of a given species [23]. Thioredoxin reductase plays a key role in catalyzing the NADPH-dependent reduction of oxidized thioredoxin to scavenge ROS, and this gene has been shown to be induced during salt stress in hulless barley [24]. Gene expression analysis in wheat revealed that most unigenes encoding peroxidase were induced by biotic stress, leading to better resistance to *Bipolaris sorokiniana* [25]. In the current study, transcriptome analysis revealed that the gene expression levels of glutathione S-transferase and glutathione synthetase, which both scavenge ROS, were significantly up-regulated in the pyroxsulam-resistant highland barley genotype. In addition, metabolite analysis revealed that the metabolite glutathione is uniquely induced in the tolerant highland barley after treatment with pyroxsulam. These results demonstrate that genes associated with the antioxidant system were up-regulated, which led to accumulation of antioxidants and subsequent scavenging of ROS in the tolerant highland barley variety. Our results shed new light on the molecular mechanisms underlying variable pyroxsulam tolerance in highland barley, and are an important first step in the development of tolerant crops through gene editing or traditional breeding. The research to promote sustainability and productivity of an important economic crops highland barley and more efficiently develop resistant crops through gene modifcation, molecular breeding, or novel genetic-editing technologies.

Declarations

Ethics approval and consent to participate

Qing 0160 and Qing 0305 were collected from Xining City, Qinghai Province, China□N.36.434419□ E.101.450759□.The samples were identified by Liling Jiang and deposited at the National duplicate Genbank for crops, Xining, Qinghai province, China. The specimen accession number were ZDM1651 and ZDM 8091. The authors declare that they comply with the IUCN Policy Statement on Research Involving Species at Risk of Extinction and the Convention on the Trade in Endangered Species of Wild Fauna and Flora.

Consent for publication

Not applicable.

Availability of data and materials

The datasets used and/or analysed during the current study are available from the corresponding author on reasonable request.

Competing interests

The authors declare that they have no competing interests

Funding

This research was funded by CAS “Light of West China”Program.

Authors’ contributions

YC and HW conceived the study and designed the experiments. HW and ZG carried out the experiments. HW, YC, ZG and HY analyzed the data. HW wrote the manuscript and draw charts and Figs. HY guided and revised the article. All authors read and approved the final manuscript.

Acknowledgements

Not applicable.

References

1. He, T. and J.F. Jia, *High frequency plant regeneration from mature embryo explants of highland barley (Hordeum vulgare L. var. nudum Hk. f.) under endosperm-supported culture.* Plant Cell Tissue and Organ Culture, 2008. **95**(2): p. 251-254.
2. Baik, B.K. and S.E. Ullrich, *Barley for food: Characteristics, improvement, and renewed interest.* Journal of Cereal Science, 2008. **48**(2): p. 233-242.

3. Newman, C.W. and R.K. Newman, *A brief history of barley foods.* Cereal Foods World, 2006. **51**(1): p. 4-7.
4. Li, Y.L., et al., *Indigenous knowledge and traditional conservation of hulless barley (Hordeum vulgare) germplasm resources in the Tibetan communities of Shangri-la, Yunnan, SW China.* Genetic Resources and Crop Evolution, 2011. **58**(5): p. 645-655.
5. Obadi, M., J. Sun, and B. Xu, *Highland barley: Chemical composition, bioactive compounds, health effects, and applications.* Food Research International, 2021. **140**.
6. Idehen, E., Y. Tang, and S.M. Sang, *Bioactive phytochemicals in barley.* Journal of Food and Drug Analysis, 2017. **25**(1): p. 148-161.
7. Jabusch, T.W. and R.S. Tjeerdema, *Chemistry and fate of triazolopyrimidine sulfonamide herbicides.* Rev Environ Contam Toxicol, 2008. **193**: p. 31-52.
8. Gonzalez, M.A., et al., *Process development for the sulfonamide herbicide pyroxsulam.* Organic Process Research & Development, 2008. **12**(2): p. 301-303.
9. Fischer, G., *Recent advances in 1,2,4-triazolo[1,5-a]pyrimidine chemistry.* Advances in Heterocyclic Chemistry, Vol 128, 2019. **128**: p. 1-101.
10. Powles, S.B. and Q. Yu, *Evolution in Action: Plants Resistant to Herbicides.* Annual Review of Plant Biology, Vol 61, 2010. **61**: p. 317-347.
11. Green, J.M. and M.D.K. Owen, *Herbicide-Resistant Crops: Utilities and Limitations for Herbicide-Resistant Weed Management.* Journal of Agricultural and Food Chemistry, 2011. **59**(11): p. 5819-5829.
12. Gulden, R.H., et al., *Conventional vs. Glyphosate-Resistant Cropping Systems in Ontario: Weed Control, Diversity, and Yield.* Weed Science, 2009. **57**(6): p. 665-672.
13. Green, J.M., *Evolution of Glyphosate-Resistant Crop Technology.* Weed Science, 2009. **57**(1): p. 108-117.
14. Djamei, A., et al., *Metabolic priming by a secreted fungal effector.* Nature, 2011. **478**(7369): p. 395-8.
15. Tanaka, S., et al., *A secreted Ustilago maydis effector promotes virulence by targeting anthocyanin biosynthesis in maize.* Elife, 2014. **3**: p. e01355.
16. Dong, N.Q., et al., *UDP-glucosyltransferase regulates grain size and abiotic stress tolerance associated with metabolic flux redirection in rice.* Nat Commun, 2020. **11**(1): p. 2629.
17. Aliferis, K.A., D. Faubert, and S. Jabaji, *A metabolic profiling strategy for the dissection of plant defense against fungal pathogens.* PLoS One, 2014. **9**(11): p. e111930.
18. Bechtold, U., et al., *Time-Series Transcriptomics Reveals That AGAMOUS-LIKE22 Affects Primary Metabolism and Developmental Processes in Drought-Stressed Arabidopsis.* Plant Cell, 2016. **28**(2): p. 345-366.
19. Casati, P. and V. Walbot, *Differential accumulation of maysin and rhamnosylisoorientin in leaves of high-altitude landraces of maize after UV-B exposure.* Plant Cell and Environment, 2005. **28**(6): p. 788-799.

20. Ferreyra, M.L.F., S.P. Rius, and P. Casati, *Flavonoids: biosynthesis, biological functions, and biotechnological applications.* Frontiers in Plant Science, 2012. **3**.
21. Kidd, P.S., et al., *The role of root exudates in aluminium resistance and silicon-induced amelioration of aluminium toxicity in three varieties of maize (Zea mays L.).* J Exp Bot, 2001. **52**(359): p. 1339-52.
22. Gill, U.S., et al., *Metabolic flux towards the (iso)flavonoid pathway in lignin modified alfalfa lines induces resistance against Fusarium oxysporum f. sp. medicaginis.* Plant Cell Environ, 2018. **41**(9): p. 1997-2007.
23. Caverzan, A., et al., *Defenses Against ROS in Crops and Weeds: The Effects of Interference and Herbicides.* Int J Mol Sci, 2019. **20**(5).
24. Lai, Y., et al., *Integrative Transcriptomic and Proteomic Analyses of Molecular Mechanism Responding to Salt Stress during Seed Germination in Hulless Barley.* Int J Mol Sci, 2020. **21**(1).
25. Ye, W., et al., *Disclosure of the Molecular Mechanism of Wheat Leaf Spot Disease Caused by Bipolaris sorokiniana through Comparative Transcriptome and Metabolomics Analysis.* Int J Mol Sci, 2019. **20**(23).

Figures

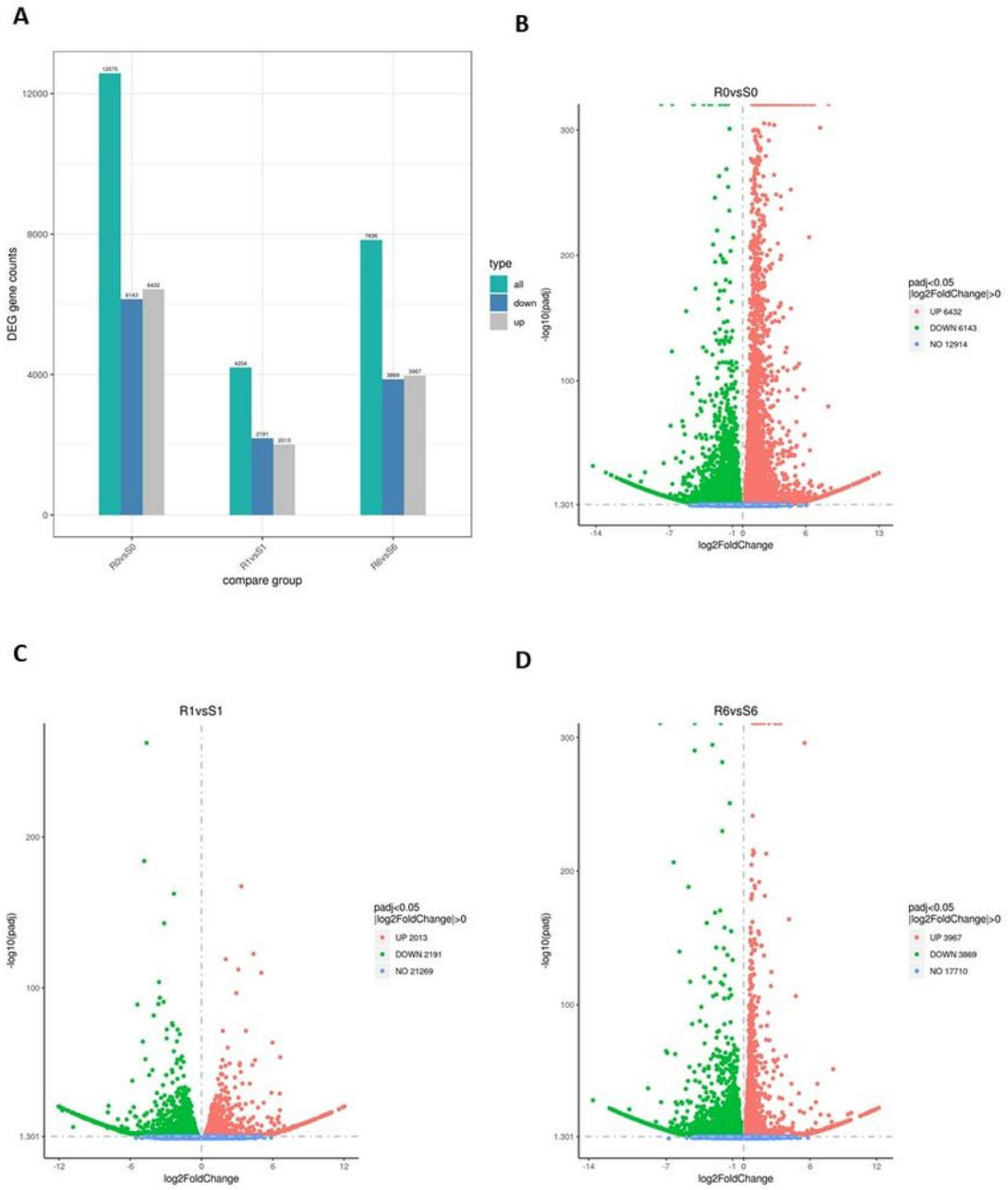

Figure 1

The number of DEGs down- and upregulated in the resistant and sensitive highland barley genotypes after pyroxsulam treatment. A. DEG counts of highland barley transcriptomes. B, C and D. Volcano maps of DEGs in the R0vsS0, R1vsS1 and R6vsS6 groups, respectively.

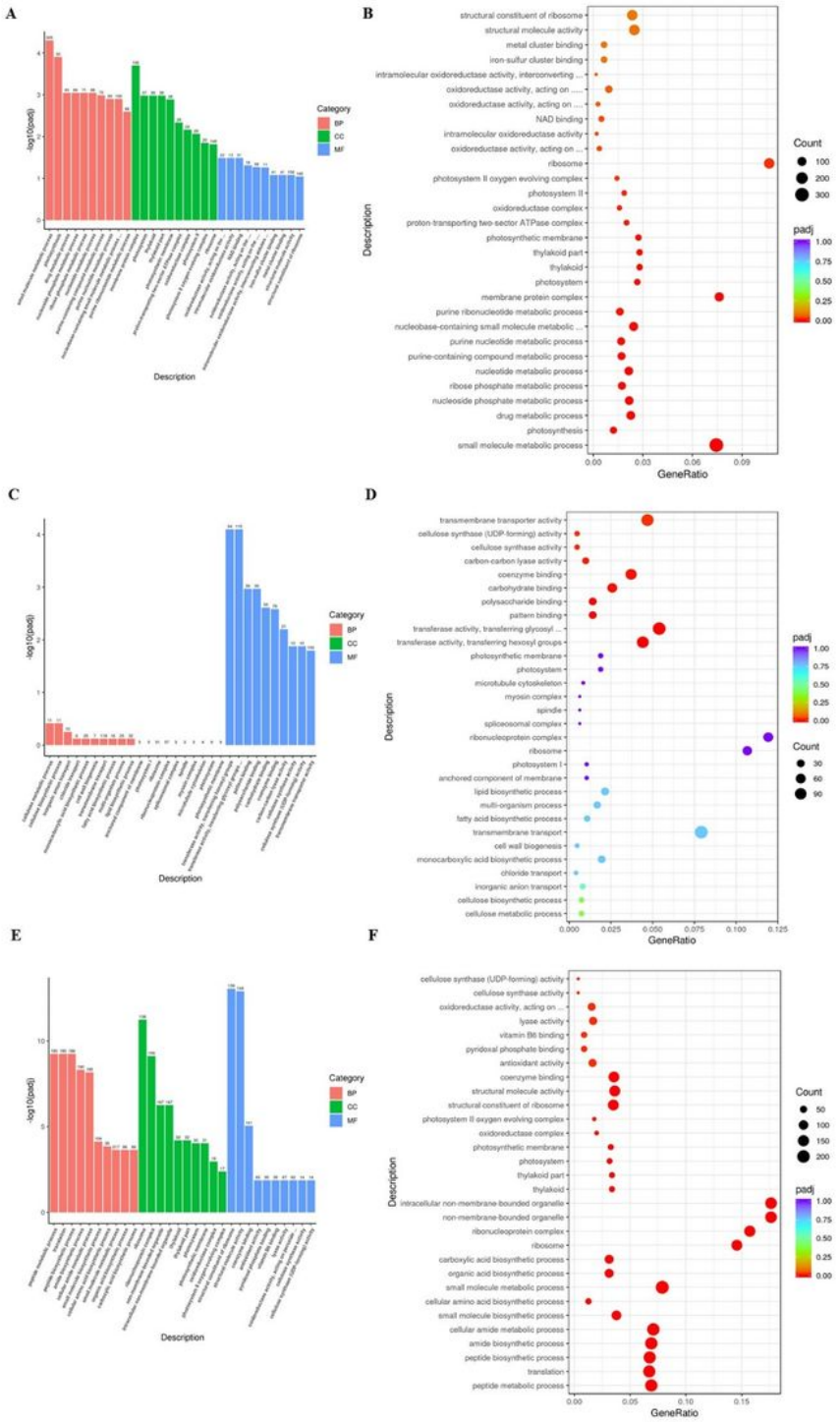

Figure 2

GO functional classification of the DEGs identified in this study. A, C and E. Differential GO enrichment between the R0vsS0, R1vsS1 and R6vsS6 transcriptomes. B, D and F. Significant GO enrichment in R0vsS0, R1vsS1 and R6vsS6, respectively.

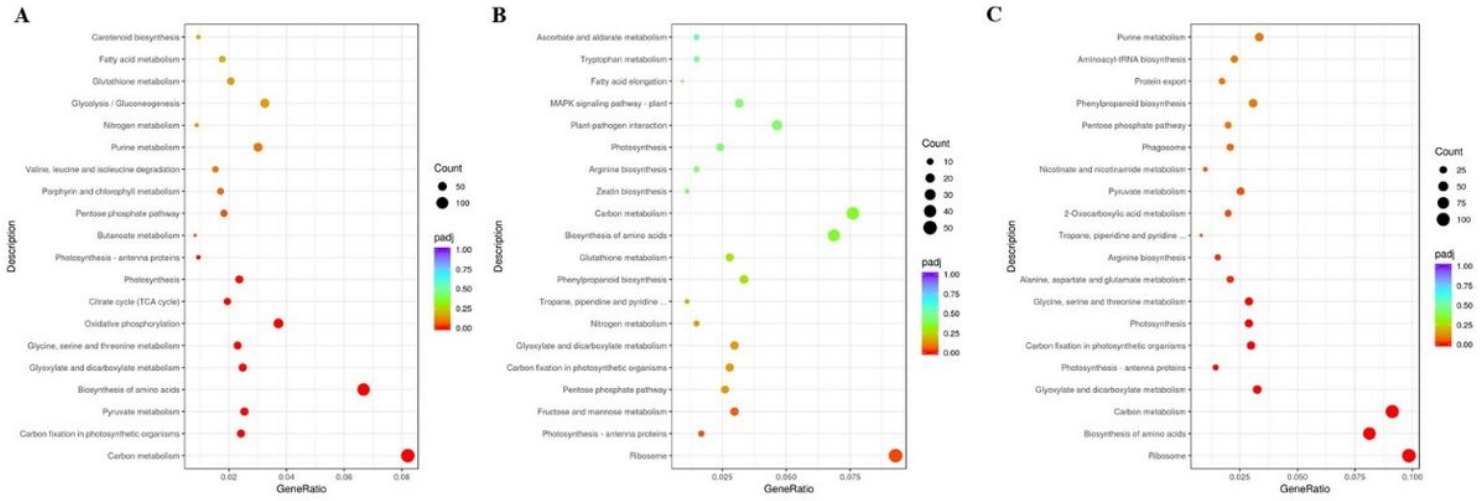

Figure 3

KEGG Pathway classification of DEGs in highland barley. The most significant KEGG pathways in the R0vsS0 group (A), R1vsS1 group (B) and R6vsS6 group (C).

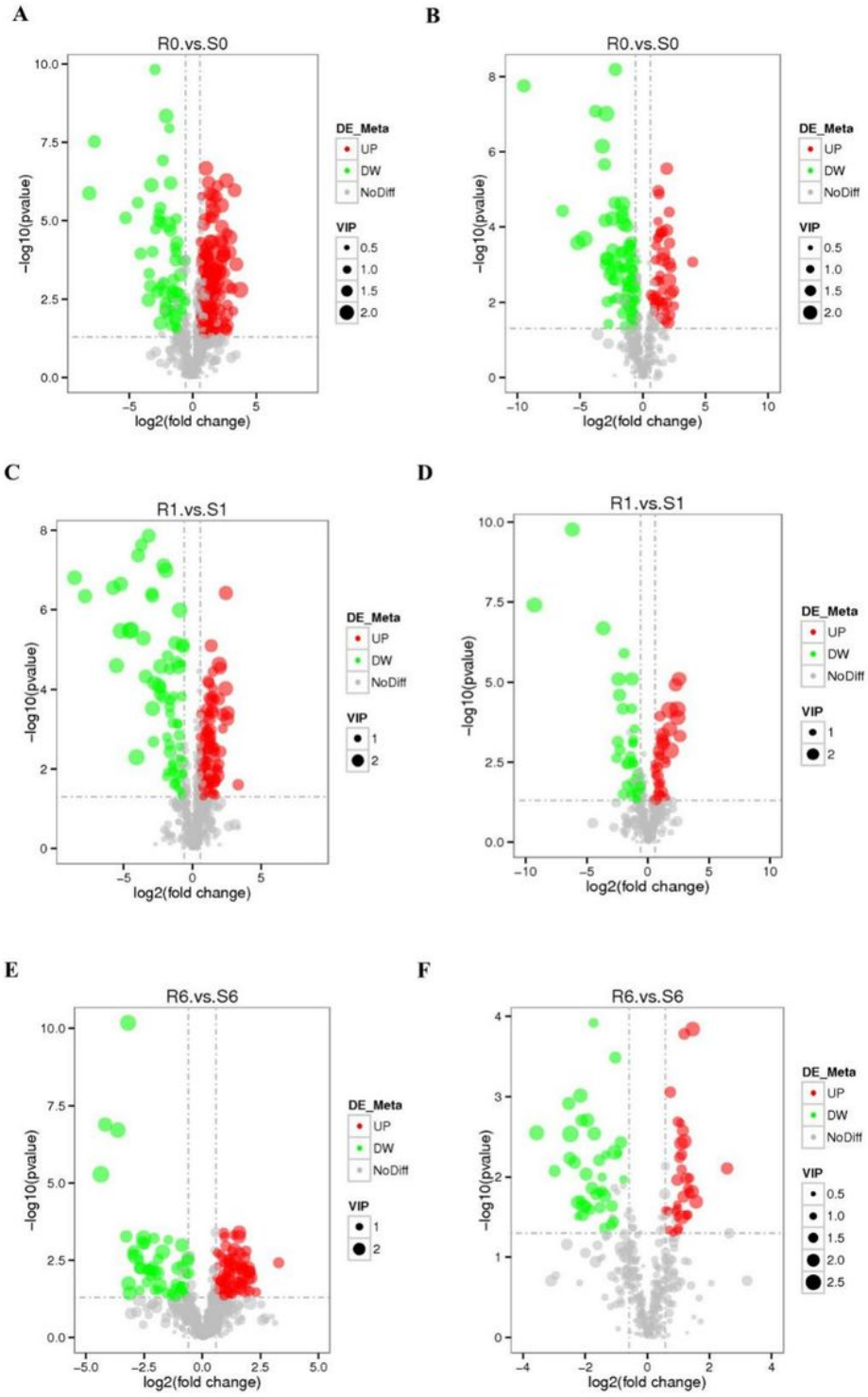

Figure 4

Differential metabolite volcano plot. The left frame is the positive ion mode, while the right frame is the negative ion mode. The abscissa represents the fold change of metabolites in different groups (log2FoldChange) and the ordinate represents the significance level of the difference (-log10p-value). Each point in the volcano plot represents a metabolite, and the significantly up-regulated metabolites are

marked with red dots, while significantly down-regulated metabolites are represented by green dots. The size of the dot represents the VIP value.

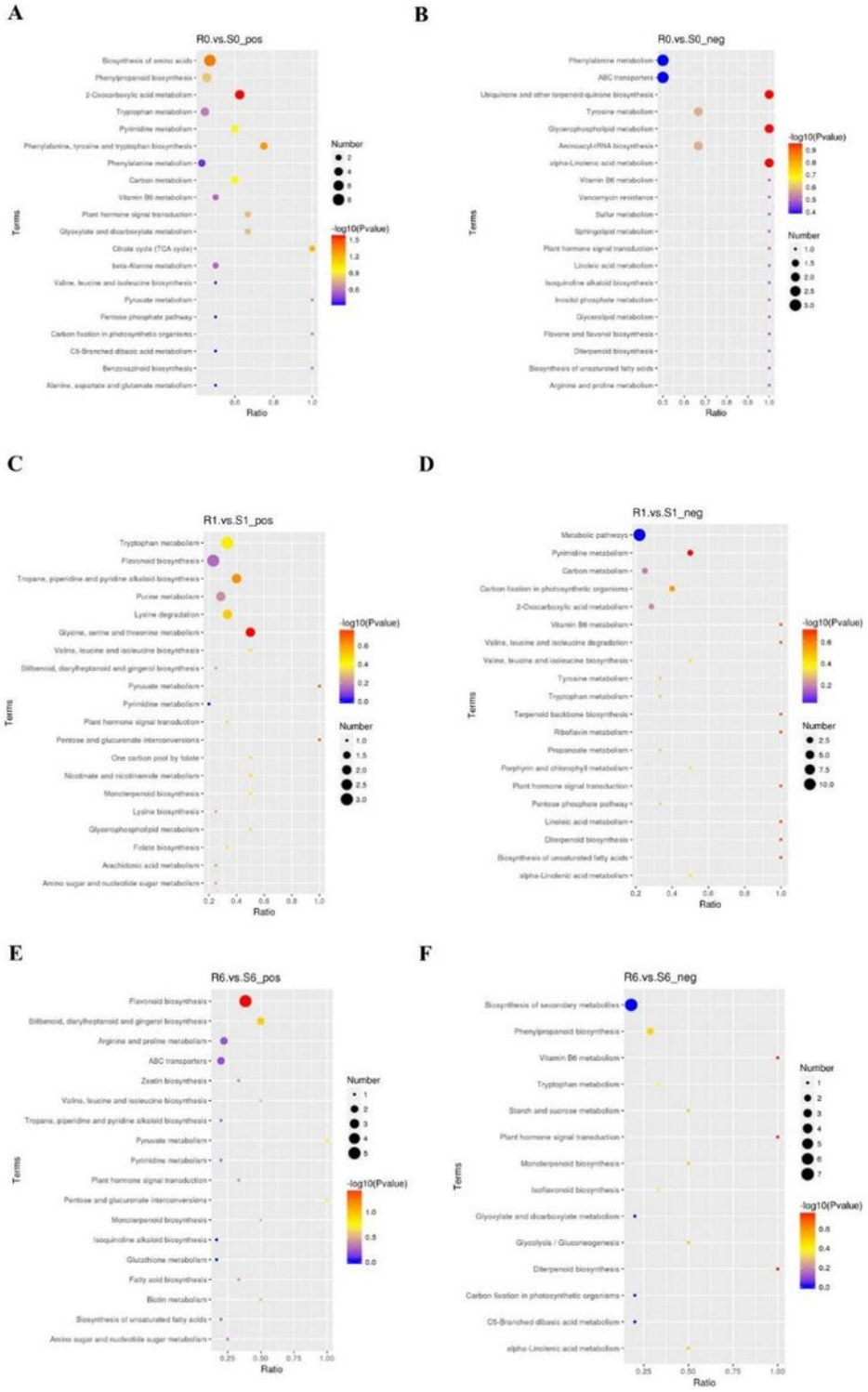

Figure 5

Differential metabolite KEGG enrichment. The left frame is the positive ion mode and the right frame is the negative ion mode. The abscissa is the ratio of the number of differential metabolites in the corresponding metabolic pathway to the total number of metabolites identified in the pathway. The larger

the value, the higher the enrichment of differential metabolites in the pathway. The color of the dot represents the P-value of the hypergeometric test. The smaller the value, the greater the reliability of the test and the more statistically significant it is. The size of the dot represents the number of different metabolites in the corresponding pathway. The larger the dot, the more differential metabolites in the pathway. The most significant differential metabolites in the KEGG pathway in R0vsS0 group (A&B), R1vsS1 group (C&D) and R6vsS6 group (E&F).

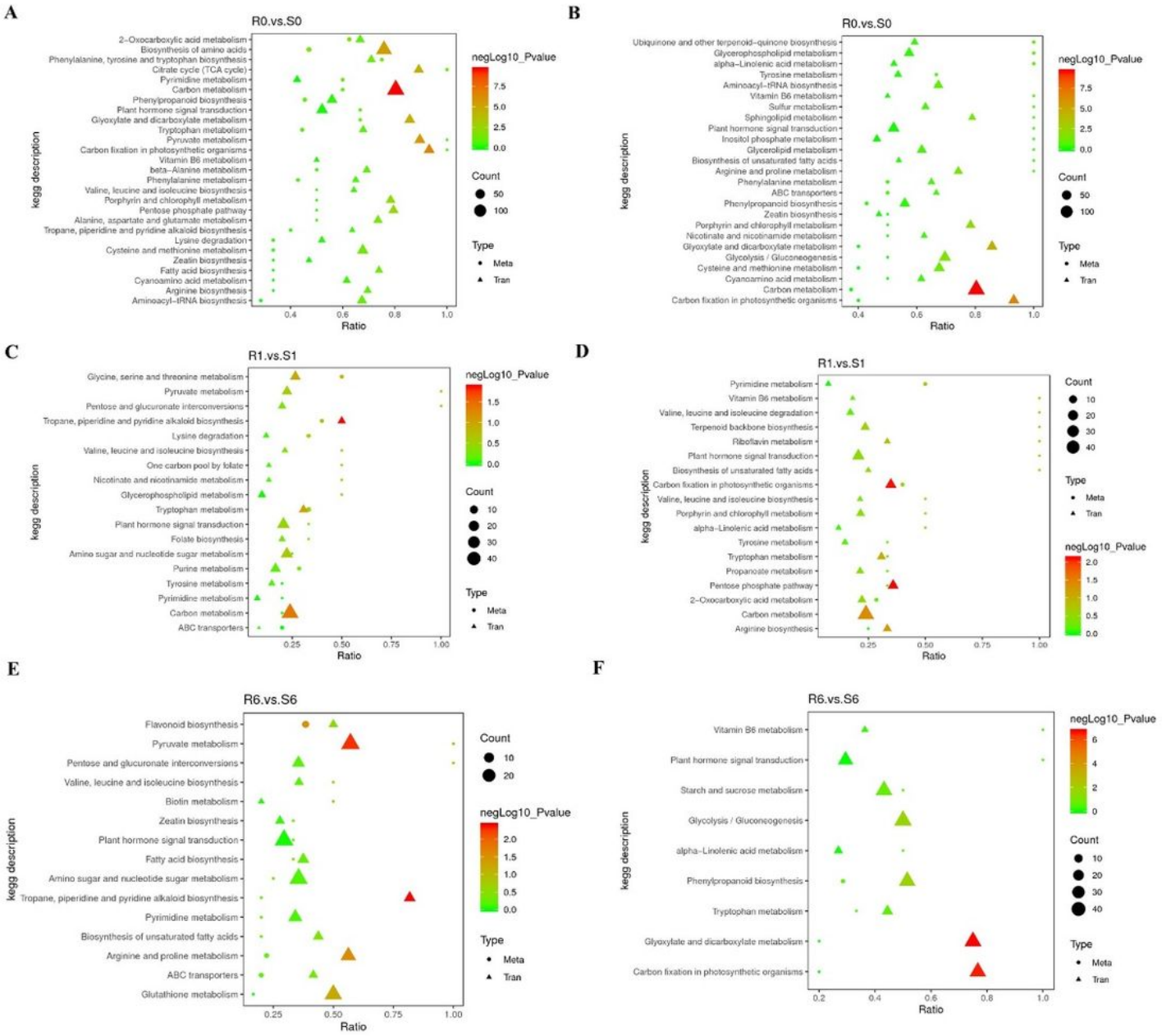

Figure 6

Correlation analysis of differentially expressed genes and differential metabolites in different KEGG pathways. The left frame is the positive ion mode, and the right frame is the negative ion mode). The abscissa is the ratio of the differential metabolites or differentially expressed genes enriched in the pathway to the number of metabolites or genes annotated in the pathway, and the ordinate is the common enrichment of metabolome-transcriptome. The count is the number of metabolites or genes enriched in the pathway.

Supplementary Files

This is a list of supplementary files associated with this preprint. Click to download.

- Supplementaryinformation.docx